

**NASA Technical Memorandum 104637**

1N-24  
66604  
32 pgs

# **Hygrothermal Properties of Composites**

**Petar Arsenovic**

**June 1996**



**NASA Technical Memorandum 104637**

# **Hygrothermal Properties of Composites**

**Petar Arsenovic**  
*Goddard Space Flight Center*  
*Greenbelt, Maryland*



National Aeronautics and  
Space Administration

**Goddard Space Flight Center**  
Greenbelt, Maryland 20771

1996

This publication is available from the NASA Center for Aerospace Information,  
800 Elkridge Landing Road, Linthicum Heights, MD 21090-2934, (301) 621-0390.

## Contents

---

<u>Section</u>	<u>Page</u>
Abstract .....	3
Section I. Introduction .....	3
Section II. Moisture Absorption and Desorption .....	5
Section III. Coefficient of Thermal Expansion .....	8
Section IV. Summary .....	14
Section V. References .....	14
Section VI. Figures .....	15

## Abstract

The testing procedure and acceptance criteria for outgassing selection of materials to be used in spacecraft has been reviewed. Outgassing testing should be conducted according to ASTM Standard E 595-90. In general, materials with CVCM  $\leq 0.10\%$  and TML  $\leq 1.00\%$  are acceptable for space applications. Next, test data on several types of graphite-epoxy composite materials are presented over time at various relative humidity levels at room temperature for moisture absorption, and under vacuum at several temperatures for moisture desorption (outgassing). The data can be accurately represented by simple equations which are useful for materials characterization. Finally, a laser dilatometer systems of extremely high sensitivity and accuracy was assembled and used to measure the coefficient of thermal expansion (CTE) of several types of graphite-epoxy structures, culminating in the ability to perform loading and thermal expansion tests on a prototype optical bench.

## Section I. Introduction

The design of modern spacecraft has posed evermore stringent demands on materials. Advanced composites with unique properties have shown great promise to meet such demands. For example, composites have been selected for spacecraft structures, optical benches and instruments due to their high modulus, high strength and dimensional stability. Numerous successful applications of composites in spacecraft have been summarized in Reference 1.

Composites have been increasingly used in the construction of many types of aircraft and spacecraft. Their light weight and high strength make the use of composites highly attractive under many circumstances. However, unlike metals, graphite-epoxy composites must be used with particular discretion in space applications because of their outgassing properties. For example, the outgassing materials may cause serious contamination problems. Thermoset and thermoplastic materials tend to be outgassers, especially at increased temperatures or in vacuum. They may emit gases and water vapors which would deposit, for instance, on lenses, mirrors and other parts of optical instruments and adversely affect their performance. This technical memorandum presents an overview of the testing procedure and acceptance criteria for outgassing selection of spacecraft materials. The test results of moisture absorption and desorption of several composite systems are discussed.

Another reason why the use of graphite-epoxy composites is so beneficial is the ability to tailor their coefficient of thermal expansion (CTE) by variations in lay-up and fiber volume. The CTE can be set to closely match that of surrounding materials to minimize thermal stresses caused by CTE mismatch. Alternatively, on systems requiring extreme thermal stability such as platforms upon which will be mounted high precision optics, it is desirable to have the CTE of the composite as near zero as possible. Presented here is an overview of the testing procedure and results for measuring the CTE of several composite systems.

The ASTM Standard E595-90 (Ref. 2) is commonly used for conducting outgassing tests for space applications. The test utilizes a "microvolatile condensable system" which mainly consists of isolated sample and collector chambers. Samples are heated to 125 °C for 24 hours in a vacuum jar to

accelerate the outgassing process. Note that testing the materials in vacuum is compatible with their use in space environment. The outgas products in each sample chamber travel through a hole to a corresponding collector chamber, wherein a portion of the outgas products will condense on a collector plate which is maintained at 25 °C. Test results are determined from the condensed materials and the total amount of outgas material from the samples. After testing in vacuum, the samples may be kept in 50% relative humidity at 25 °C for 24 hours for an optional test to determine the amount of water reabsorbed by each sample. It is termed as water vapor regained (WVR) and expressed as a percentage of sample mass before the test. Because of the micro-quantities involved in the tests all procedures detailed in the ASTM Standard should be followed closely so as to obtain consistent and accurate results.

Referring to the above, the mass of condensate on the collector plate is calculated as a percentage of the mass of the original sample; this is the collected volatile condensible material (CVCM). Also, the total mass of material outgassed from the sample is determined by measuring the sample before and after the test. The total mass loss (TML) due to outgassing is expressed as a percentage of the initial sample mass. In general, materials which have  $CVCM \leq 0.10\%$  and  $TML \leq 1.00\%$  as specified in ASTM E595-90 are acceptable for space applications.

Goddard Space Flight Center (GSFC) has extensive experience in the study of outgassing properties of materials for spacecraft applications. A wealth of GSFC test data has been made available to the space industry through a series of NASA publications over a period of some 20 years. The latest is *NASA Reference Publication 1124, Revision 3*, which includes GSFC outgassing data on many materials generated through July 1993 (Ref. 3). The data are also available through the Materials and Processing Technical Information Service (MAPTIS) data bank at Marshall Space Flight Center, Huntsville, Alabama.

Although the outgassing data from Reference 3 or other sources can greatly facilitate the selection of materials for use in spacecraft, such test data should still be examined for each application to make sure that they are suitable for the particular functions and design requirements of the spacecraft.

Sometimes outgassing data from different sources on one composite material may disagree with each other although they all have used the same ASTM Standard test method. This is quite possible for a number of reasons. For example, if the samples were taken from different batches with some slight variations in the manufacturing process they could have different outgassing properties; and this could happen even though the variations were all within the producer's specifications. For this reason, after a composite is selected for space application, it is still necessary to perform outgassing test on each batch of the material for quality control purposes.

In case a selected composite has all the preferred properties for a particular application except for outgassing, a thermal-vacuum treatment may be used to remove its outgassing materials. Also, some modifications in materials processing, such as a suitable change in the cure cycle, may bring about sufficient improvement. If no method sufficiently reduces its outgassing the composite should be replaced by an alternate material, or it may be used with some shielding or venting devices to protect the instruments from contamination.

## Section II: Moisture Absorption / Desorption

### Experimental Procedure

The first composite system tested was T50/ERL1962 graphite-epoxy coupons of thickness roughly 20 mils. For moisture absorption, twelve samples were thoroughly baked out at 90 °C for 120 hours and then placed in different environments with respect to humidity in groups of three. The mass of each coupon was measured periodically over time at each humidity level with a high precision Ohaus analytical microbalance having a readability to 0.00001 grams. The coupons were exposed to 21%, 38%, 65%, and 100% relative humidity at 25 °C.

Moisture desorption testing was accomplished by first preconditioning a set of graphite-epoxy coupons at 80 °C in an environment of 100% humidity for a period of 670 hours to ensure that the specimens were fully saturated with water. Following this, a Cahn vacuum balance was used to record the mass loss over time of the samples under a vacuum of  $10^{-5}$  Torr at temperatures of 40, 60, and 90 °C.

Experimental data on moisture absorption of this graphite-resin system are summarized in figure 1. The vertical coordinate represents the average mass gains of specimens in three tests in each of the four different relative humidity levels. The mass gain is defined as the measured increase in mass of a specimen during exposure to controlled humidity and expressed as a percentage of the initial mass of the dry specimen. Figure 1 shows that moisture absorption started with high rates which decreased quickly in low humidity and gradually in high humidity. Each curve appears to level off eventually toward a point of saturation which is dependent on the relative humidity.

It is interesting to note that the mass gain versus time curves become linear in log-log coordinates with approximately the same slope as shown in figure 2. Therefore, an empirical equation can be established for the tested composite as

$$M = kt^{0.33}$$

where       $M$  = mass gain, %  
               $t$  = time, h

The quantity  $k$  is a function of relative humidity and is equal to the mass gain at unit time. Figure 3 shows that a plot of  $\log H$  versus  $\log k$  is linear. Thus,

$$k = (H/1238.40)^{0.85}$$

where  $H$  is the relative humidity. After substitution into Equation 1, the overall moisture absorption behavior can be described by

$$M = (H/1238.40)^{0.85} t^{0.33}$$

This equation is simple and accurate, and represents the experimental data reasonably well, although not perfectly, as seen in figure 1.

Test data for moisture desorption are presented in figure 4. The vertical coordinate represents the mass loss which is expressed as a percentage of the initial mass of the specimens after preconditioning in 100% relative humidity. Figure 4 shows that moisture desorption started with high rates which decreased quickly at high temperature and gradually at low temperature. The curves appear to level off eventually to a point when the coupons would be completely dry. It is interesting to note that the maximum mass loss is about the same magnitude of the mass gain shown in figure 1. This indicates that all the moisture absorbed in the composite could outgas as water vapor in vacuum.

The moisture desorption data can be analyzed by a diffusion model (Ref. 4) as follows:

$$m = m_t[1 - \exp(-7.3(t/t_c)^{0.75})]$$

where  $m$  = mass loss, %  
 $m_t$  = total change in mass, %  
 $t$  = time, h  
 $t_c$  = characteristic time, h

The change in mass, i.e., mass loss, is related to the "characteristic" time, which is in turn a function of the diffusion parameters. Thus,

$$t_c = x^2 / (D_o \exp[-Q/RT])$$

where  $x$  = thickness of the material  
 $D_o$  = diffusion constant frequency factor  
 $Q$  = activation energy  
 $R$  = gas constant  
 $T$  = absolute temperature

Based on the test data, the activation energy associated with the diffusion process is determined as  $Q=8.5$  KCal/Mol, which is within 10% of the literature values (Ref. 5). The total change in mass  $m_t$  is a parameter which is determined as  $m_t = -1.2\%$  by its best fit to the experimental data using Equation 4. The number  $m_t$  is given a negative sign to account for moisture desorption. A value of  $D_o = 0.85$  in<sup>2</sup>/hr is used. This value is also determined by the best fit to the data and is typical for an epoxy compound of this type (Ref. 5). The  $t_c$  values are calculated for the three test temperatures as follows:

T (°K)	$t_c$ (hours)
313	402
333	175
363	62



Figure 4 shows that there is a good agreement between Equation 4 and the experimental data. Deviations between experiment and the theoretical are no more than about 10%.

This section now reports on a series of graphite-epoxy specimens manufactured by COI, Ford-Dow, Lockheed, and TRW. An important concern for these graphite-epoxy composites was their stability with regard to moisture absorption and thermal cycling. It was desired to make a comparison among these different composite systems. Note that the thickness of these specimens is about 80 mils, or 4 times thicker than the previous ones. We are now dealing in time frames of a year rather than a month.

Figure 5 shows the moisture absorption for two specimens supplied by TRW; the first was a standard T300/934 graphite-epoxy coupon, and the other AS4-PEEK thermoplastic. The samples were initially baked out for 3 days to drive off moisture. They were then kept in an environment of room temperature and 100% relative humidity, and weighed periodically in a high precision balance. As can be seen from figure 5, the AS4-PEEK displayed a much smaller mass increase than the T300/934.

Figure 6 shows the moisture absorption curve for a specimen from Lockheed, designated Tonox. As before, the coupon was initially conditioned in an oven for three days to drive off moisture, and then placed into a test chamber at 100% humidity and room temperature. The Tonox showed the typical pattern of initial rapid mass gain followed by saturation.

Figure 7 shows the moisture absorption curves for six specimens from COI, 3 being P75S/ERL1962 graphite-epoxy coupons and the other 3 additionally having a moisture barrier coating of an Indium-Tin type 1E alloy. They were initially conditioned in an oven for three days to drive off moisture, then kept at 55% humidity and room temperature. As can be seen from figure 3, the samples with the coating showed a much smaller mass gain than the uncoated ones in the elapsed time of almost 600 days.

Figure 8 shows the moisture absorption curves for six specimens from Ford-Dow, 3 designated 934 and the other 3 as RS-3 polycyanate. The test conditions were the same as for the COI coupons, i.e., initial bakeout followed by environmental conditions of 55% humidity and room temperature. The results are similar to the COI specimens, with the RS-3 coupons showing a much smaller mass increase as compared to the 934 samples.

Figures 9 and 10 show moisture desorption curves for another set of COI and Ford-Dow specimens, respectively. The coupons were all initially conditioned in an environment of 100% humidity and 90 °C for a period of 4 weeks to fully saturate them with moisture. Following this, they were placed in a vacuum, and only removed for periodic weighing. All the coupons lost mass as they outgassed, with the coated samples from COI and the RS-3 samples from Ford-Dow displaying a much smaller change in mass than their respective counterparts.

### Section III: Measurement of Coefficient of Thermal Expansion

The coefficient of thermal expansion, denoted as CTE, is defined as:

$$CTE = (1/L)(dL/dT)$$

where L is the length of the specimen and T is the temperature. Conventional materials have CTE's on the order of tens of microstrains per °C, however, graphite-epoxies can have values hundreds of times smaller. Measurement of these small dimensional changes requires a dilatometer with great precision. The one that we assembled and integrated has three subsystems:

- 1) A laser interferometer, consisting of a single mode, frequency stabilized HeNe laser and control electronics. This device is a Hewlett-Packard Laser Transducer System, model 551. It can measure the displacement of a corner reflector to a resolution of 0.6 microinches, over a working distance of up to 200 feet.
- 2) A CompuAdd 386 PC-compatible computer using an IEEE bus to communicate with the laser transducer system. The computer also collects and stores the data for analysis.
- 3) An environmental chamber consisting of a thick walled stainless steel tube in an insulating box. Heating and cooling are managed by attached thermocouples, along with a Keithley 740 Scanning Thermometer system and thermal controllers, and electrical heaters and fluid circulation tubes. The chamber can handle temperatures from 25 to 300 degrees Celsius with a high degree of uniformity and stability.

The laser beam is split into two beams by an optical beam splitter, and impacts on two corner reflectors mounted on opposite ends of the specimen. The beams will be reflected, recombined, and detected by a receiver. Heating causes a change in length of the test specimen, thus changing the traveling distance of the reflected beam. The length of the sample is directly proportional to the number of wavelengths of light reflected. The control electronics stabilizes the frequency of the laser beam to within 1 part in  $10^7$ . The change in the number of wavelengths of reflected light is counted by the detector, which sends this data to the computer. Software written in HP Basic computes change in length from data received by the detector. By knowing this value, the temperature range that was used, and the original length of the sample, the CTE can be calculated. A computer plot is generated for each specimen tested of change in temperature vs. change in length. The CTE is the slope of the curve divided by the original length of the sample. The final step in the calculation is making a correction for the fact that the experiments are performed in air, not vacuum. The index of refraction of the laser beam in air varies with temperature, as the air's density is changing. It is necessary to add a correction factor of  $0.9 \times 10^{-6}/^{\circ}\text{C}$  to the calculated CTE. We will now show this mathematically:

The distance D is measured by the number of wavelengths of light contained in it:

$$N = D / \lambda$$

where  $\lambda$  is the wavelength of the light. Since we work in air, then the wavelength is that in air, which is related to the wavelength in a vacuum by

$$\lambda_{\text{air}} = \lambda_{\text{vac}} / n$$

where  $n$  is the refractive index of air. The refractive index of air depends on the amount of air present, and on the detailed composition of the air including its water content, which is usually measured by the relative humidity. We find theoretically that

$$n = 1 + \sum Z_s M_s$$

where  $Z_s$  is the polarizability of the gas of species  $s$ , and  $M_s$  is the number of moles per volume of the species  $s$ . For our purposes, only the species  $N_2$ ,  $O_2$ , and  $H_2O$  are important. Since the ideal gas law applies with excellent precision for the components of air at normal temperatures and pressures, then

$$M_s = p_s / RT$$

where  $p_s$  is the partial pressure of the species  $s$  (the total air pressure is  $p = \sum p_s$ ),  $R$  is the ideal gas constant, and  $T$  is the absolute temperature. Hence,  $n$  changes with variations in the barometric pressure, with relative humidity, and with temperature.

Hence, the number of wavelengths contained in the distance  $D$  is

$$N = D / \lambda_{\text{air}} = [D / \lambda_{\text{vac}}] n = \{D / \lambda_{\text{vac}}\} [(\sum Z_s p_s / RT)]$$

when measurements are made in air, and this number will increase as  $D$  increases and as  $n$  increases (i.e., as  $p_s$  increases or as  $T$  decreases). The vacuum wavelength is controlled with a precision of better than 1 part in  $10^8$  by the laser, which therefore may be regarded as constant for this derivation.

The interferometer measures changes in the number  $N$ :

$$\begin{aligned} C &= N_{\text{new}} - N_{\text{old}} \\ C &= [(D_{\text{new}} n_{\text{new}}) - (D_{\text{old}} n_{\text{old}})] / \lambda_{\text{vac}} \\ C &= (\Delta D n + D \Delta n) / \lambda_{\text{vac}} + \text{negligible terms} \end{aligned}$$

where  $\Delta D = D_{\text{new}} - D_{\text{old}}$  and  $\Delta n = n_{\text{new}} - n_{\text{old}}$ . Hence,  $C$  will change both when the length  $D$  changes and when the index changes, i.e., when the air pressure and the relative humidity and the air temperature change.

For the optical arrangement used with the interferometer, only the air in the sample length  $L$  affects  $C$ . (This is not true for many arrangements of other interferometers used for this purpose, where  $C$  is determined by all the air in the entire beam; such arrangements produce data that are far more

difficult to correct and interpret.) If we ignore changes in air pressure and relative humidity and assume the variation in the index is due to temperature changes, then:

$$\begin{aligned} dn/dT &= d/dT (1 + Zp/RT) = -(Zp/RT^2) \\ dn/dT &= -(T_o/T^2) (Zp/RT_o) = (T_o/T^2) (n - 1)_o \\ dn/dT &\cong \{273 \text{ K} / T^2\} (0.000291) -0.90 * 10^{-6} / ^\circ\text{C at } 25 ^\circ\text{C} \end{aligned}$$

Then:

$$dC/dT = [dD/dT] n + D [dn/dT]$$

and so we can compute both an “apparent” CTE and a true one, with the relation between them:

$$\begin{aligned} (\text{CTE})_{\text{true}} &= (1/L) (dL/DT) \\ (\text{CTE})_{\text{app}} &= \lambda C/dT \\ (\text{CTE})_{\text{true}} &= (\text{CTE})_{\text{app}} - dn/dT \\ (\text{CTE})_{\text{true}} &\cong (\text{CTE})_{\text{app}} + 0.90 * 10^{-6} / ^\circ\text{C at } 25 ^\circ\text{C} \end{aligned}$$

That is, we must add  $0.90 * 10^{-6} / ^\circ\text{C}$  to the “apparent” thermal expansion.

In practice, both changes in air pressure and relative humidity do occur while temperature cycling is in progress. The air pressure typically ranges over about +/- (3 to 5)%. The relative humidity is fairly well controlled in the laboratory, but can range from 45% to 65%. These changes can affect  $n - 1$  by roughly the same amount. These effects combined can influence the value of the correction factor by about 10%. These changes should average out over a series of runs lasting a week or more (long compared to the time for typical weather systems to move through our area).

Now, the coefficient of thermal expansion (CTE) was determined for two standard specimens. The first was a 2-inch copper rod certified by the National Institute of Science and Technology (NIST), while the other was a ten inch coupon of ULE glass certified by Corning.

Each sample was subjected to a temperature range from 25 to 60 °C. Temperature variation was performed at a rate of 2 °C per hour. Figure 11 shows the respective data of change in length versus temperature for each specimen. The graph shown is from the raw data collected from the dilatometer. As explained previously, a correction factor of 0.9 ppm/°C must be added to the CTE calculated from this data to get the final result. Table 1 shows the overall final CTE values for each sample.

**Table 1. CTE of Standards Using Laser Dilatometer**

Specimen	Manufacturer	CTE (ppm/°C) from Mfg.	CTE (ppm/°C) from laser dilatometer
Copper Cu SRM 736	NIST	17.0	16.9
ULE Glass	Corning	0.003	<0.1

The CTE values for copper were within 0.3% of each other. Corning claims the CTE of their ULE glass to be 3 ppb/°C +/- 1 ppb/°C for the temperature range tested. This is roughly two orders of magnitude finer resolution than the laser dilatometer can reasonably measure. The instrument does confirm the CTE of the glass to be within 0.1 ppm/°C of zero.

Next, we present the CTE measurements for 4 graphite-epoxy tube specimens. They had the dimensions 1.75 inches wide by 0.04 inches thick by 11 inches long. Each sample was subjected to a temperature range from 25 to 50 °C. Temperature variation was performed at a rate of 5 °C per hour. Table 2 shows the overall CTE values for each tube, while figure 12 shows the respective graphs of change in length (corrected for air effects) versus temperature for each specimen.

**Table 2. CTE of Square Tubes T50/954-2A, Layup [0/+63.5/0/-63.5]**

Tube Designation	CTE
GSFC-T99 A	$0.1 * 10^{-6}/^{\circ}\text{C}$
GSFC-T99 B	$0.0 * 10^{-6}/^{\circ}\text{C}$
GSFC-T99 C	$0.2 * 10^{-6}/^{\circ}\text{C}$
GSFC-T100 C	$-0.1 * 10^{-6}/^{\circ}\text{C}$

Finally, we present another set of data for another set of specimens as described below.

**Table 3. CTE Results for Coupon Specimens**

Samples	Layup	CTE
P40 984 Coupon 1	[0] <sub>16</sub>	$-0.2 * 10^{-6}/^{\circ}\text{C}$
P40 984 Coupon 2		$-0.1 * 10^{-6}/^{\circ}\text{C}$
P40 984 Coupon 3		$-0.7 * 10^{-6}/^{\circ}\text{C}$
P40 984 Coupon 4		$-0.3 * 10^{-6}/^{\circ}\text{C}$
P40 984 Coupon 5		$-0.2 * 10^{-6}/^{\circ}\text{C}$
P40 984 Coupon 6		$-0.5 * 10^{-6}/^{\circ}\text{C}$

Average CTE:  $-0.33 * 10^{-6}/^{\circ}\text{C} = -0.18 * 10^{-6}/^{\circ}\text{F}$

P42 985 Coupon 1	[90] <sub>16</sub>	$28.2 * 10^{-6}/^{\circ}\text{C}$
P42 985 Coupon 2		$30.0 * 10^{-6}/^{\circ}\text{C}$
P42 985 Coupon 3		$27.5 * 10^{-6}/^{\circ}\text{C}$
P42 985 Coupon 4		$29.3 * 10^{-6}/^{\circ}\text{C}$
P42 985 Coupon 5		$26.9 * 10^{-6}/^{\circ}\text{C}$
P42 985 Coupon 6		$28.7 * 10^{-6}/^{\circ}\text{C}$

Average CTE:  $28.4 * 10^{-6}/^{\circ}\text{C} = 15.8 * 10^{-6}/^{\circ}\text{F}$

**Table 3. CTE Results for Coupon Specimens (con't.)**

P45 987 Coupon 1	[0,30,90,-30]	$0.2 * 10^{-6}/^{\circ}\text{C}$
P45 987 Coupon 2		$0.1 * 10^{-6}/^{\circ}\text{C}$
P47 987 Coupon 3		$0.2 * 10^{-6}/^{\circ}\text{C}$
P47 987 Coupon 4		$0.2 * 10^{-6}/^{\circ}\text{C}$
P44 987 Coupon 5		$0.2 * 10^{-6}/^{\circ}\text{C}$
P44 987 Coupon 6		$0.1 * 10^{-6}/^{\circ}\text{C}$

Average CTE:  $0.18 * 10^{-6}/^{\circ}\text{C} = 0.10 * 10^{-6}/^{\circ}\text{F}$

We have used the laser dilatometer to test the coefficient of thermal expansion of graphite epoxy composite specimens in a variety of geometries, namely coupons, tubes, and honeycomb structures. The next logical step was to use the instrument to test an actual prototype of a composite optical bench for the Far Ultraviolet Spectrographic Explorer project. Both CTE and loading tests were performed.

The bench was prepared with metal inserts. A pillar was bolted into each insert (front and rear), with optical corner reflectors attached to the top and bottom of each pillar. Note that this employs the use of a total of four corner reflectors, as opposed to two for all the previous specimens. We used the laser dilatometer to measure changes in the distance between both the top and bottom pairs of reflectors. These changes were measured in units of  $\lambda/40$ , where  $\lambda$  is the wavelength of the light (6328 Angstroms) emitted from our He-Ne laser as described previously. The distance changes are recorded as integers, which are labeled as  $C_{top}$  and  $C_{bot}$ . These two numbers allow calculation of both the strain of the midplane of the bench and the curvature of the bench:

$$\epsilon = (\lambda/40) [(C_{top} - \delta C_{bot}) / (L \{1-\delta\})]$$

$$1/R = (\lambda/40) [(C_{top} - C_{bot}) / (L h_{top} \{1-\delta\})]$$

where R is the radius of curvature of the midplane of the bench, L is the distance between the posts,  $h_{top}$  is the distance between the midplane of the bench and the top corner reflector,  $h_{bot}$  is the distance between the central plane of the bench and the bottom corner reflector, and  $\delta = h_{bot} / h_{top}$ .

The dimensions of this particular model bench were:

$$\begin{aligned} L &= 51.7 \text{ cm.} \\ h_{top} &= 24.7 \text{ cm.} \\ h_{bot} &= 6.92 \text{ cm.} \end{aligned}$$

The load testing was conducted by placing a series of lead weights close to the center of the bench. Each had a mass of 2.4 kilograms. The loading sequence was as follows:

- measure the undisturbed bench for a few minutes to establish a baseline
- place a single weight on the bench and leave it there for at least 20 seconds; long enough for the computer data logger to get at least 10 records
- remove the weight and leave the bench undisturbed for at least 20 seconds, to measure the extent to which the bench returns to the original shape
- repeat this sequence for 2 weights, 3 weights, and 4 weights

As seen in figure 13, the changes in the distances between the top corner reflectors  $C_{top}$  and between the bottom reflectors  $C_{bot}$ , were linear with applied load to within the scatter of the measurements. The scatter of these measurements amounted to better than 1 part in 3000, and the correlation coefficients were all above 0.999. There was no detectable hysteresis to within this accuracy. Each individual loading cycle followed Hooke's law to the limits of detection of the instrument.

If the bench were not symmetric about the midplane, then we might expect that a load  $M$  would produce a midplane strain  $\epsilon$  :

$$\epsilon = B M$$

where  $B$  is a constant that relates strain to loading. But the maximum loading did not deform the midplane length of the bench to within the small uncertainty of these measurements. That is, center loading of the bench in this manner produced pure bending only, and no midplane stretching or compression. This experimentally confirmed what was theoretically expected.

One measure of the extent of bending is the "radius of curvature"  $R$ . We find that

$$1 / R = A M$$

where  $A$  is a constant that relates bending to loading. The results of four separate series of tests were:

Test	A in units of $10^{-7} / (\text{cm kg})$
#1	1.841
#2	1.828
#3	1.834
#4	1.846
Avg.	1.837

While the midplane strain introduced by the center loading tests was below the limit of resolution of these measurements, the strain introduced at the top and bottom face sheets differed from zero by hundreds of times their uncertainties; it was about 4 microstrains at the maximum load. Since the faceplate materials do not fail until strained to roughly 0.4%, the top and bottom plates had a safety factor of roughly 1000 at the maximum load used in these tests.

For thermal expansion testing, the bench was enclosed within a thermal chamber with heaters at its top and bottom. Each heater was monitored with its own thermocouple, and attached to its own temperature controller, which had a resolution of  $\pm 1^\circ\text{C}$  in temperature and 1 second in time. The temperature was cycled linearly from 25 to 75  $^\circ\text{C}$  at a rate of 1 cycle per day. The CTE was almost constant as a function of temperature, with the average CTE being  $0.96 \times 10^{-6}/^\circ\text{C}$ .

#### **Section IV: Summary**

The testing procedure and acceptance criteria for outgassing selection of materials to be used in spacecraft has been reviewed. Outgassing testing should be conducted according to ASTM Standard E 595-90. In general, materials with CVC  $\leq 0.10\%$  and TML  $\leq 1.00\%$  are acceptable for space applications.

Test data on several types of graphite-epoxy composite materials are presented over time at various relative humidity levels at room temperature for moisture absorption, and under vacuum at several temperatures for moisture desorption (outgassing). The data can be accurately represented by simple equations which are useful for materials characterization.

A laser dilatometer system of extremely high sensitivity and accuracy was used to measure the CTE of several types of graphite-epoxy structures, culminating in the ability to perform loading and thermal expansion tests on a prototype optical bench.

#### **Section V: References**

1. V. P. McConnell, "Progress Report: Composites in Space", Advanced Composites, July/August 1991, p.26.
2. ASTM Standard E 595-90, Standard Test Method for Total Mass Loss and Collected Volatile Condensable Materials from Outgassing in a Vacuum Environment, Annual Book of ASTM Standards, Vol. 15.03, American Society for Testing and Materials, 1992.
3. W. A. Campbell, Jr., and J. J. Scialdone, "Outgassing Data for Selecting Spacecraft Materials", NASA Reference Publication 1124, Revision 3, September 1993.
4. G. S. Springer, "Environmental Effects, Section 16 in Composite Design, 4th Edition, Edited by S. W. Tsai", Think Composites, 1988.
5. C. Barrett, W. Nix, and A. Tetelman, "The Principles of Engineering Materials", Prentice Hall, 1973.



---

---

## Figures

---

---

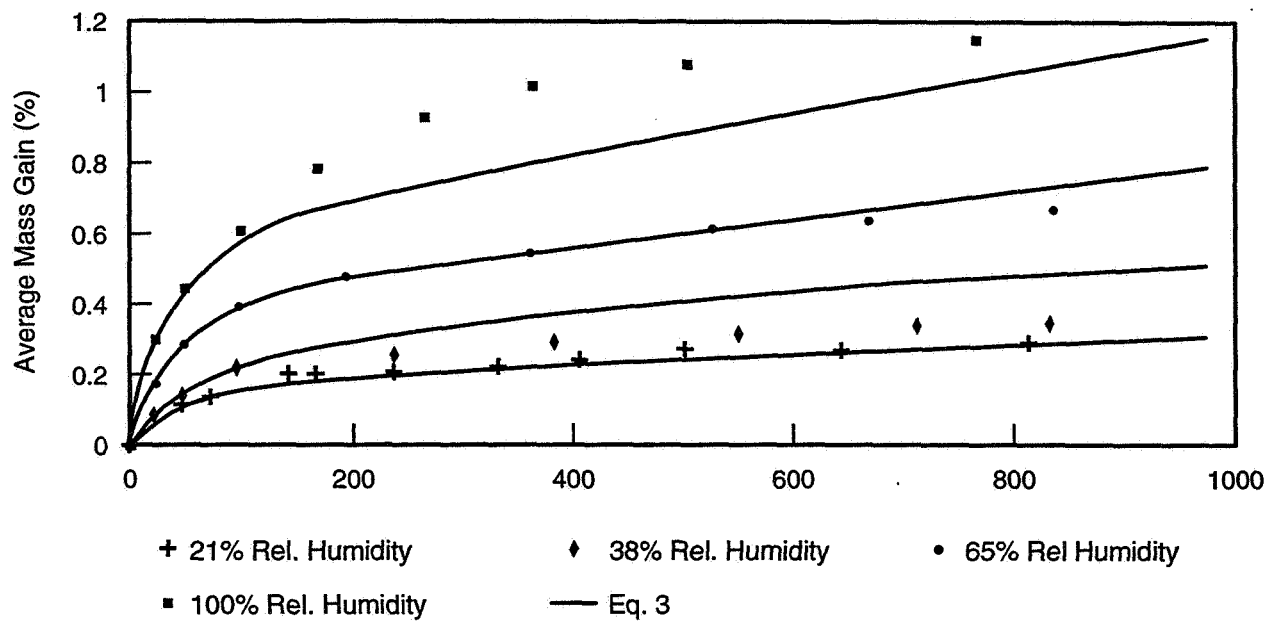


Figure 1. Moisture absorption of T50/ERL 1962 at four relative humidity levels

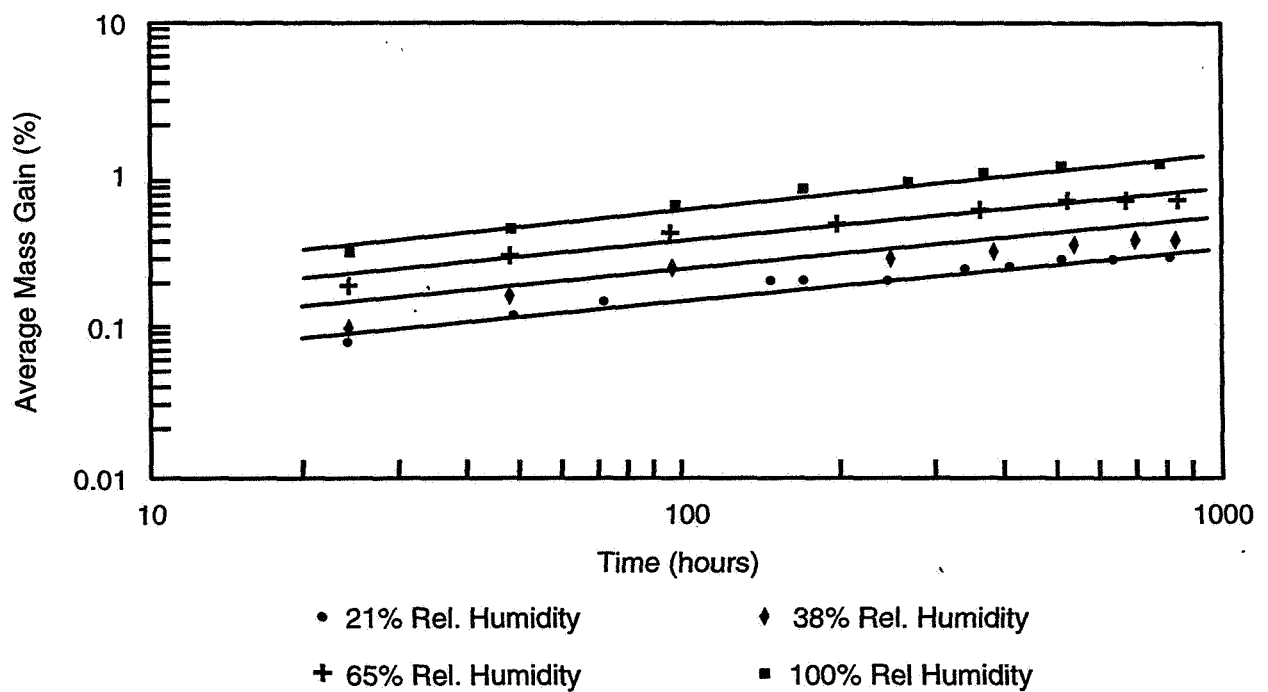


Figure 2. Log-Log plot of moisture absorption data on T50/ERL 1962

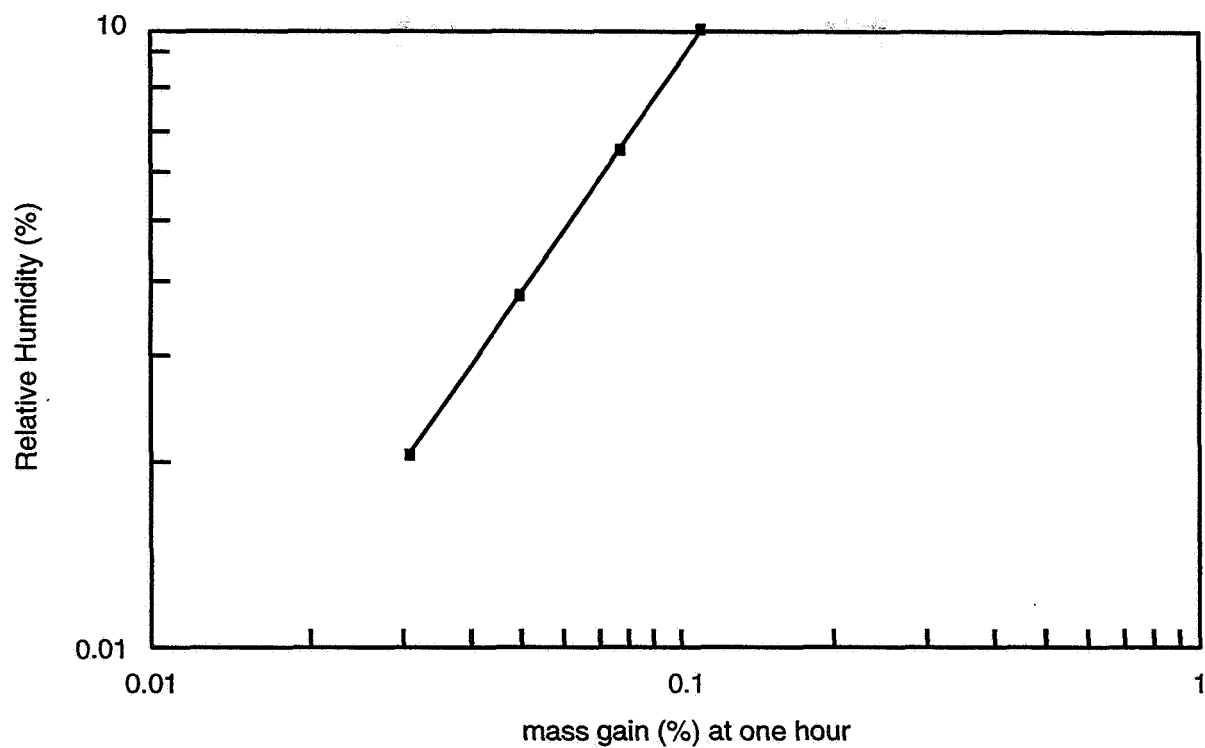


Figure 3. Moisture absorption data on T50/ERL 1962 at unit time.

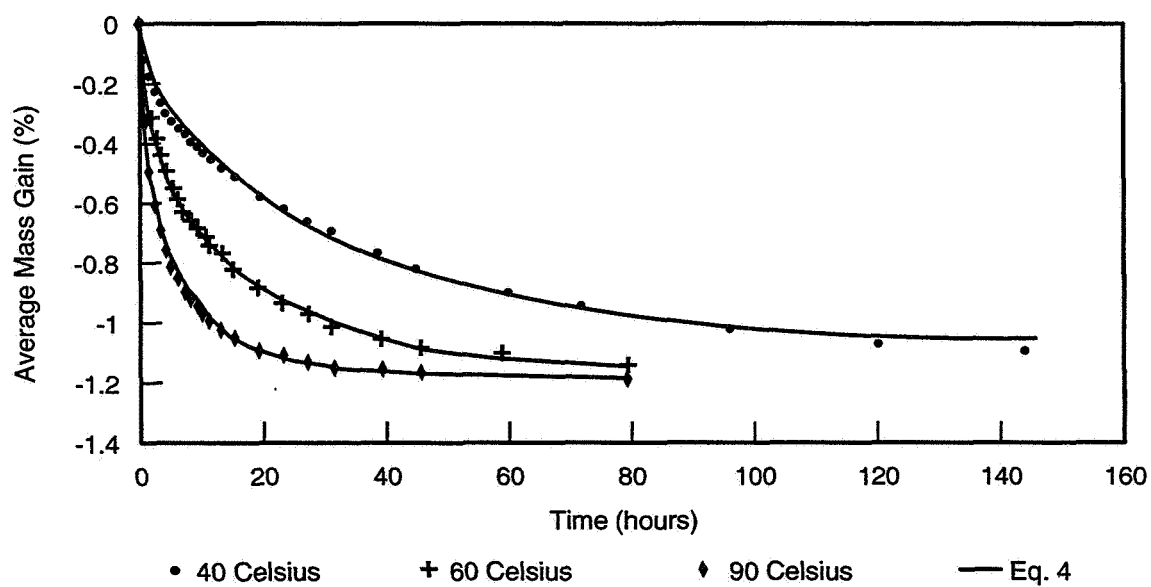


Figure 4. Moisture desorption of T50/ERL 1962 at three temperatures

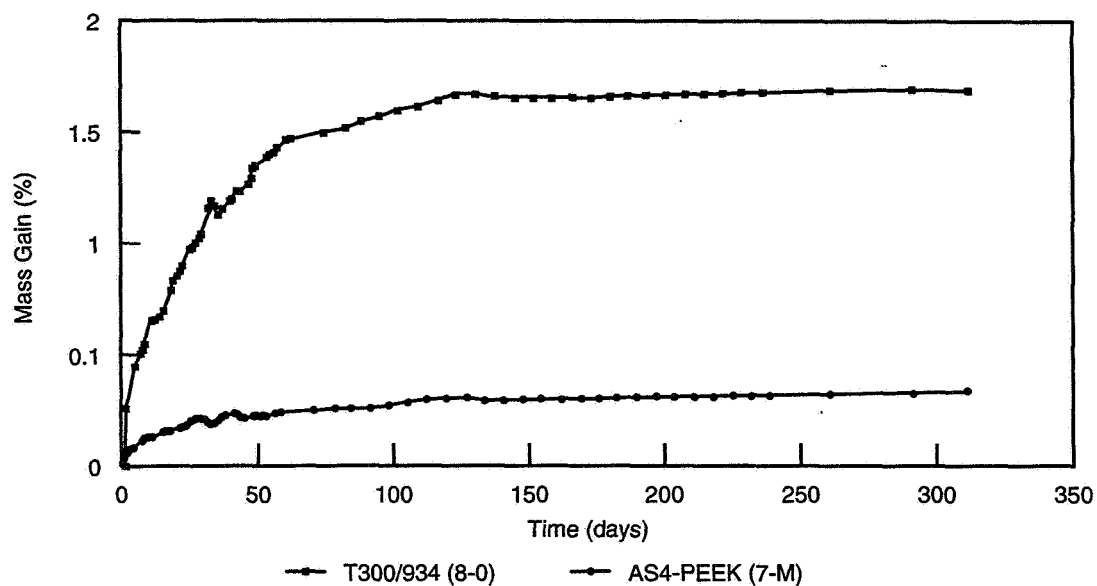


Figure 5. Moisture absorption of TRW specimens at 100% relative humidity

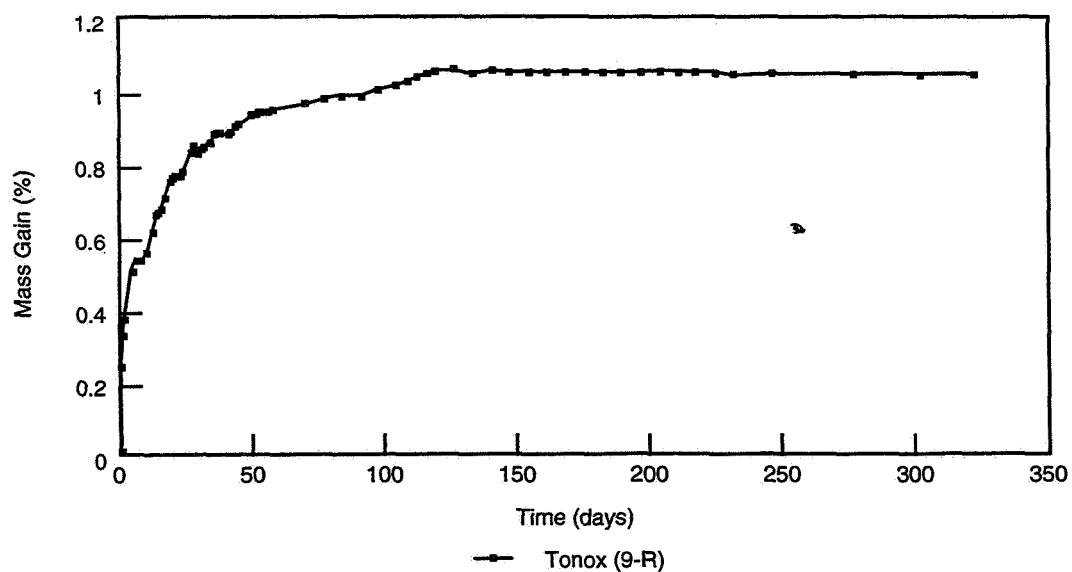


Figure 6. Moisture absorption of Lockheed specimen at 100% relative humidity

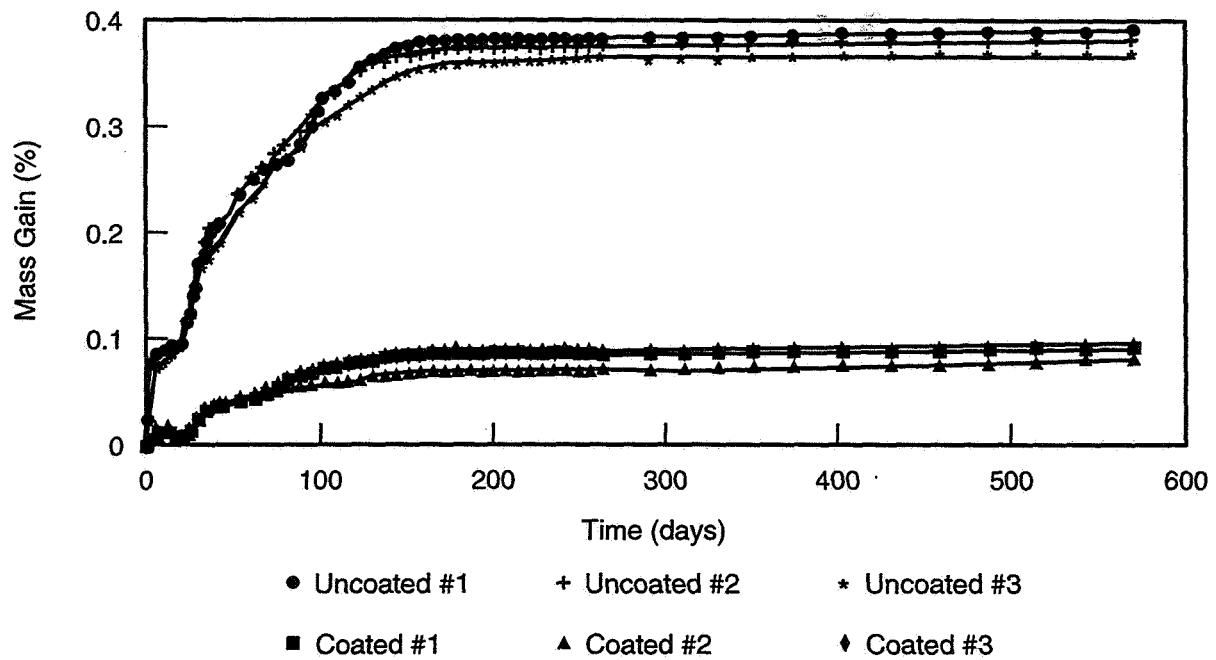


Figure 7. Moisture absorption of COI specimens at 55% relative humidity

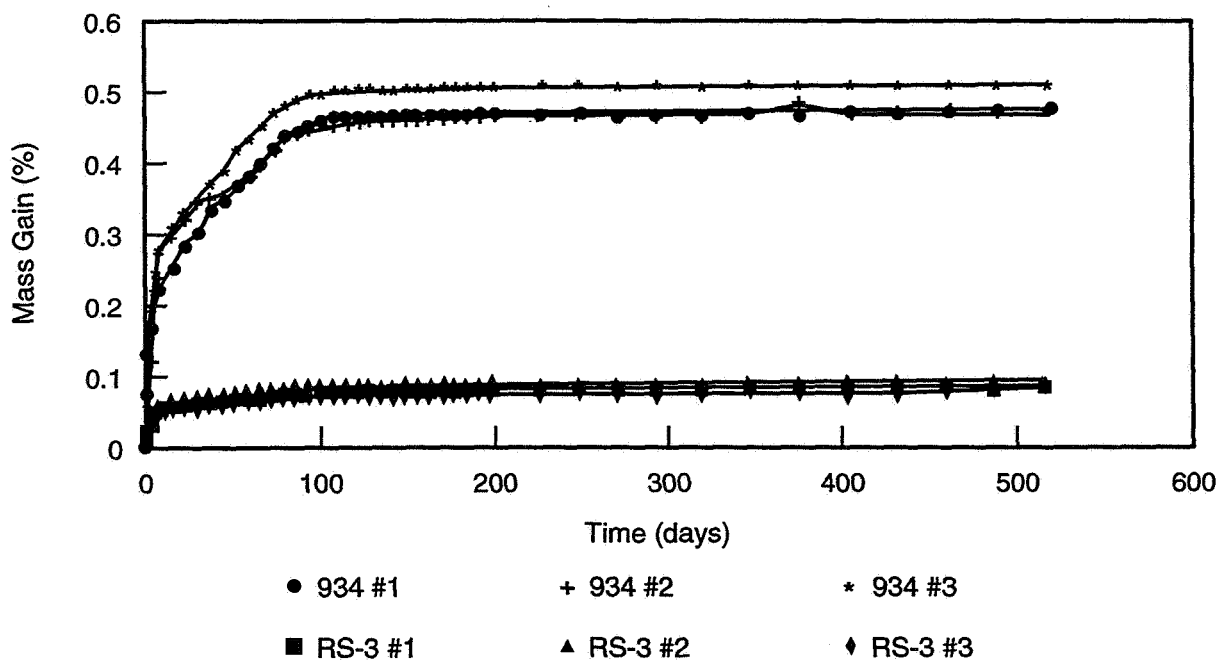


Figure 8. Moisture absorption of Ford-Dow specimens at 55% relative humidity

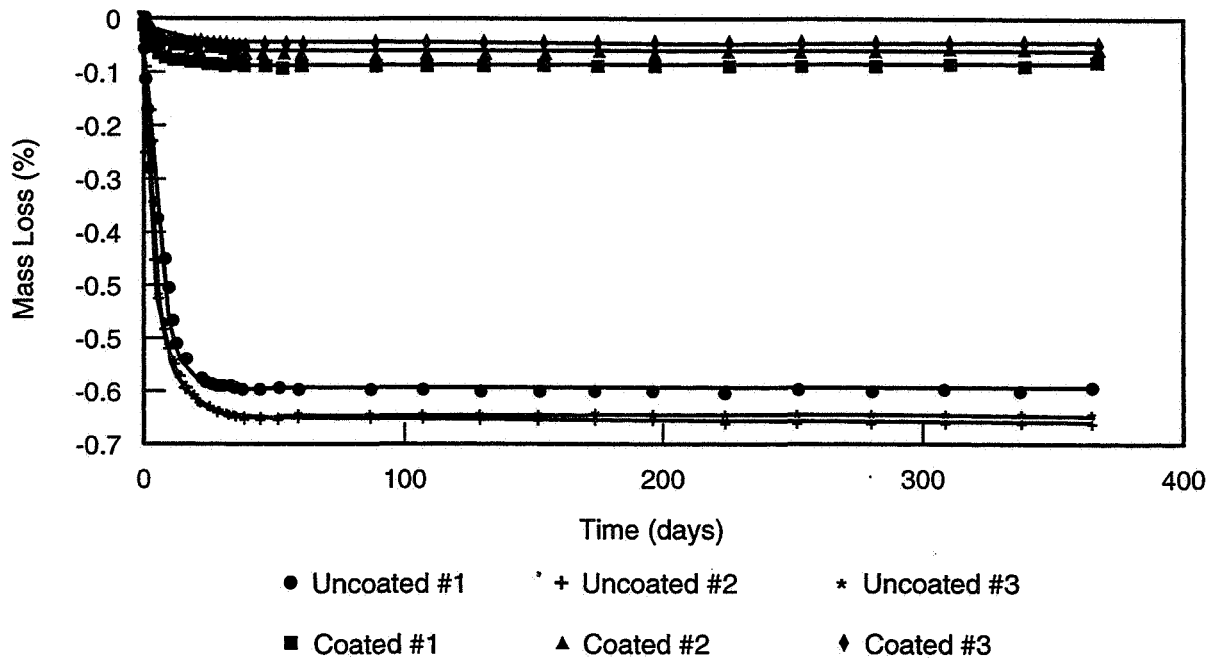


Figure 9. Moisture desorption of CIO specimens at room temperature

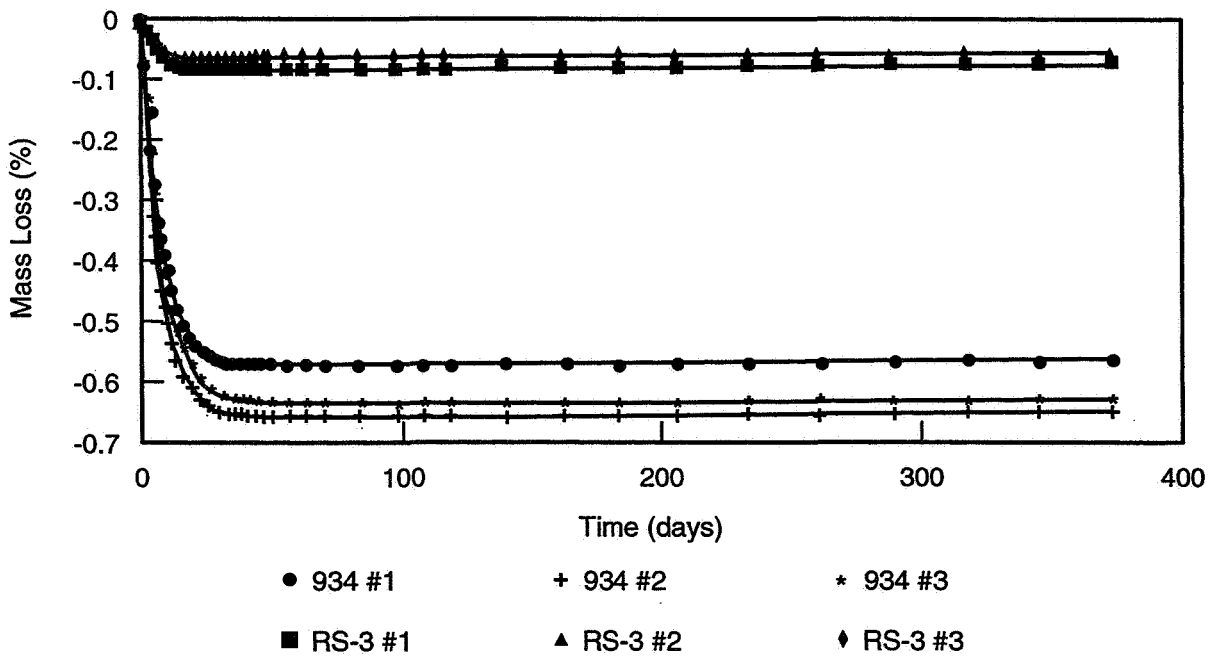


Figure 10. Moisture desorption of Ford-Dow specimens at room temperature

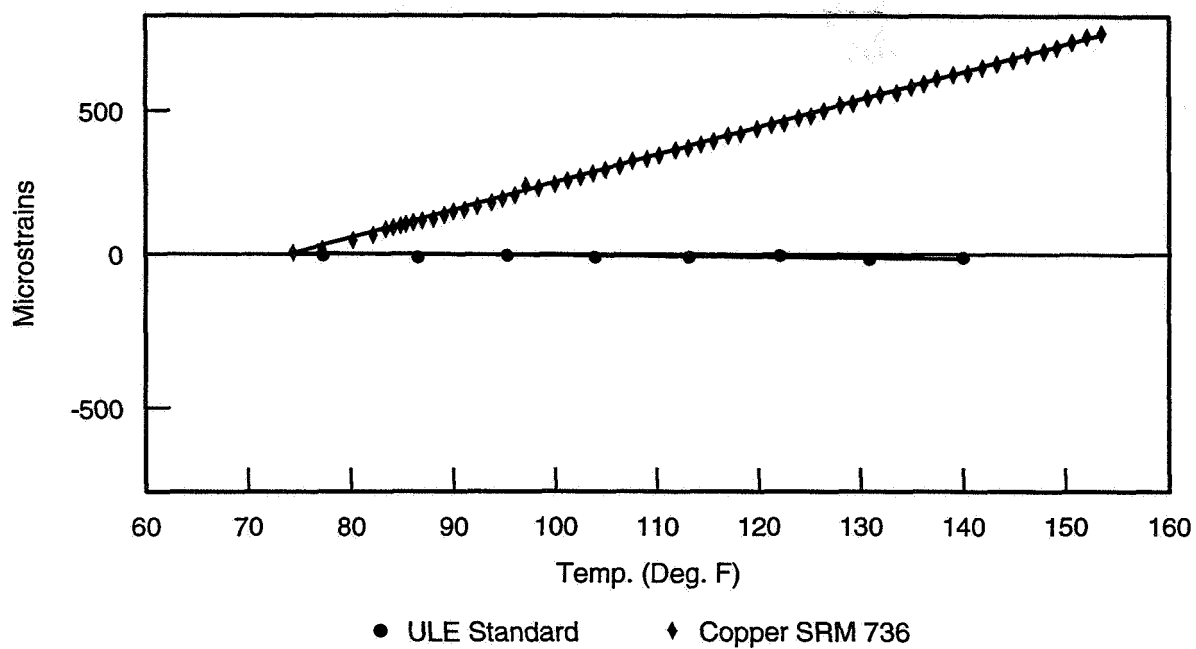


Figure 11. CTE of copper and ULE standards

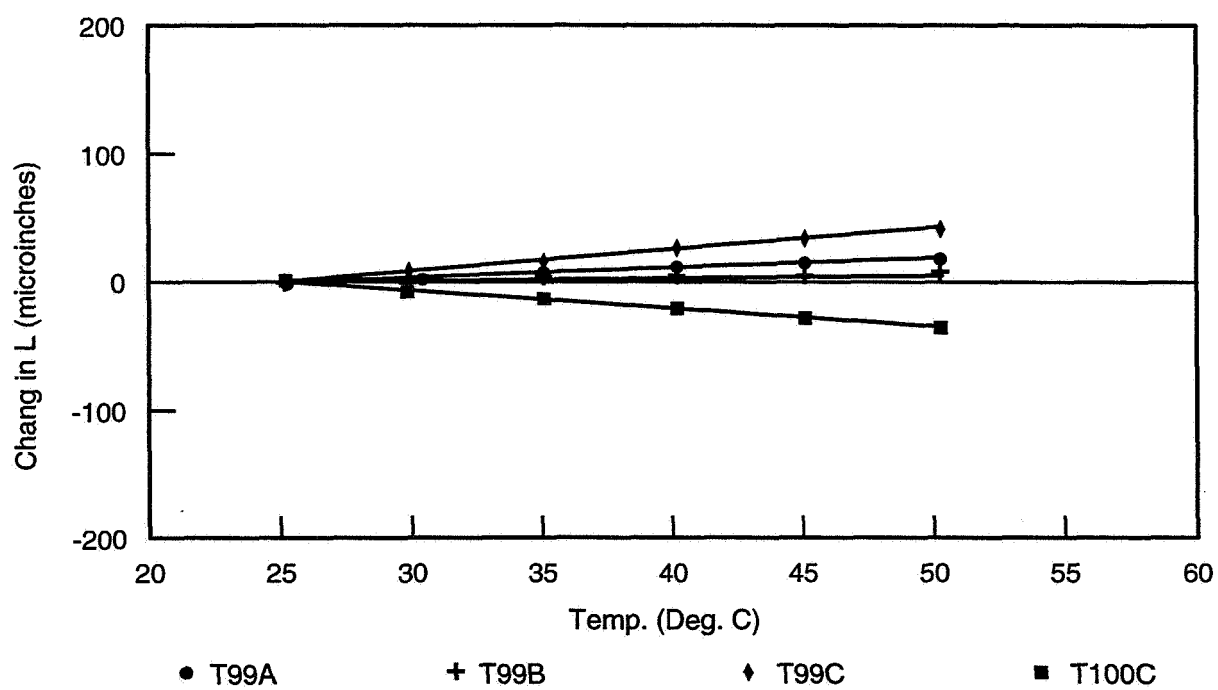


Figure 12. CTE of composite tubes

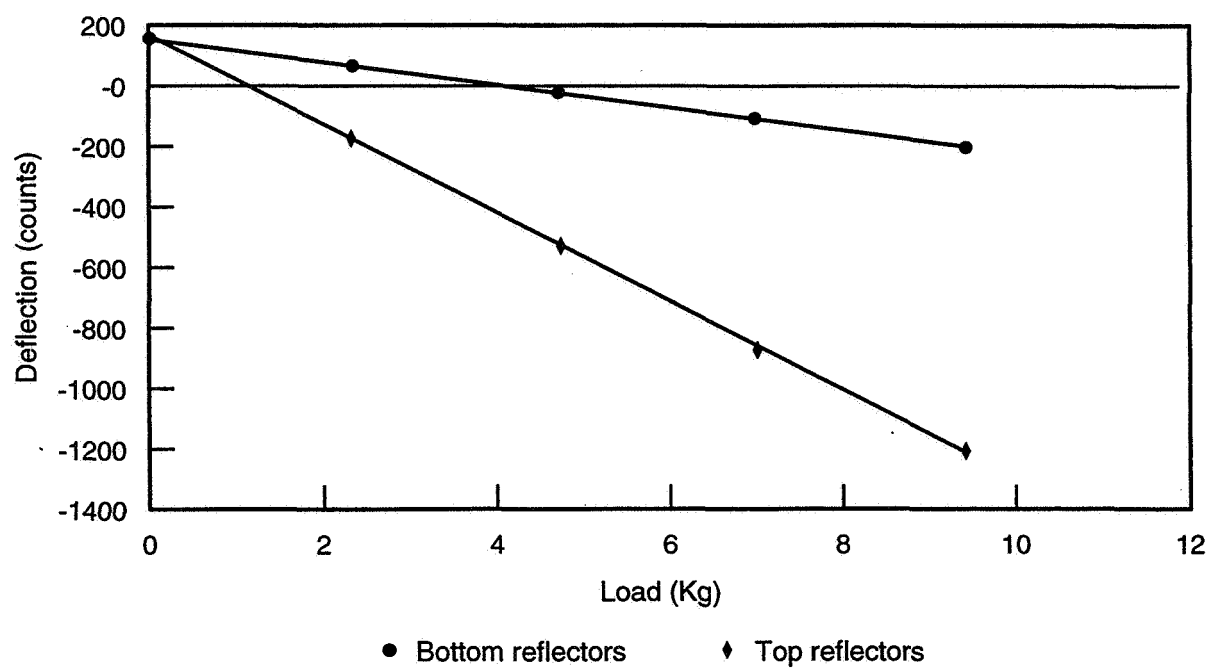


Figure 13. Load vs. Deflection for prototype optical bench



**REPORT DOCUMENTATION PAGE**Form Approved  
OMB No. 0704-0188

Public reporting burden for this collection of information is estimated to average 1 hour per response, including the time for reviewing instructions, searching existing data sources, gathering and maintaining the data needed, and completing and reviewing the collection of information. Send comments regarding this burden estimate or any other aspect of this collection of information, including suggestions for reducing this burden, to Washington Headquarters Services, Directorate for Information Operations and Reports, 1215 Jefferson Davis Highway, Suite 1204, Arlington, VA 22202-4302, and to the Office of Management and Budget, Paperwork Reduction Project (0704-0188), Washington, DC 20503.

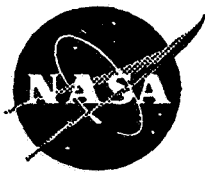
<b>1. AGENCY USE ONLY (Leave blank)</b>		<b>2. REPORT DATE</b> June 1996	<b>3. REPORT TYPE AND DATES COVERED</b> Technical Memorandum	
<b>4. TITLE AND SUBTITLE</b>  Hygrothermal Properties of Composites			<b>5. FUNDING NUMBERS</b>  Code 313	
<b>6. AUTHOR(S)</b>  Petar Arsenovic				
<b>7. PERFORMING ORGANIZATION NAME(S) AND ADDRESS(ES)</b>  Goddard Space Flight Center Greenbelt, Maryland 20771			<b>8. PERFORMING ORGANIZATION REPORT NUMBER</b>  96B00089	
<b>9. SPONSORING/MONITORING AGENCY NAME(S) AND ADDRESS(ES)</b>  NASA Aeronautics and Space Administration Washington, D.C. 20546-0001			<b>10. SPONSORING/MONITORING AGENCY REPORT NUMBER</b>  TM-104637	
<b>11. SUPPLEMENTARY NOTES</b>				
<b>12a. DISTRIBUTION/AVAILABILITY STATEMENT</b>  Unclassified-Unlimited Subject Category: 24 Report available from the NASA Center for AeroSpace Information, 800 Elkridge Landing Road, Linthicum Heights, MD 21090; (301) 621-0390.			<b>12b. DISTRIBUTION CODE</b>	
<b>13. ABSTRACT (Maximum 200 words)</b>  The testing procedure and acceptance criteria for outgassing selection of materials to be used in spacecraft has been reviewed. Outgassing testing should be conducted according to ASTM Standard E 595-90. In general, materials with CVCM $\leq$ 0.10% and TML $\leq$ 1.00% are acceptable for space applications. Next, test data on several types of graphite-epoxy composite materials are presented over time at various relative humidity levels at room temperature for moisture absorption, and under vacuum at several temperatures for moisture desorption (outgassing). The data can be accurately represented by simple equations which are useful for materials characterization. Finally, a laser dilatometer systems of extremely high sensitivity and accuracy was assembled and used to measure the coefficient of thermal expansion (CTE) of several types of graphite-epoxy structures, culminating in the ability to perform loading and thermal expansion tests on a prototype optical bench.				
<b>14. SUBJECT TERMS</b>  composite, laser, microstrain, thermal			<b>15. NUMBER OF PAGES</b>  22	
			<b>16. PRICE CODE</b>	
<b>17. SECURITY CLASSIFICATION OF REPORT</b>  Unclassified	<b>18. SECURITY CLASSIFICATION OF THIS PAGE</b>  Unclassified	<b>19. SECURITY CLASSIFICATION OF ABSTRACT</b>  Unclassified	<b>20. LIMITATION OF ABSTRACT</b>  Unlimited	

**National Aeronautics and  
Space Administration**

**Goddard Space Flight Center  
Greenbelt, Maryland 20771**

**Official Business  
Penalty for Private Use, \$300**

**SPECIAL FOURTH-CLASS RATE  
POSTAGE & FEES PAID  
NASA  
PERMIT No. G27**



**POSTMASTER: If Undeliverable (Section 158,  
Postal Manual) Do Not Return**

---